Developmental Biology **252,** 59–71 (2002)
doi:10.1006/dbio.2002.0834

Patterning through Differential Endoreduplication in Epithelial Organogenesis of the Chordate, *Oikopleura dioica*

Philippe Ganot and Eric M. Thompson[1]

Sars International Centre for Marine Molecular Biology, Bergen High Technology Centre, Thormøhlensgt. 55, N-5008 Bergen, Norway

The contributions that control of cell proliferation and cell growth make to developmental regulation of organ and body size remain poorly explored, particularly with respect to endocycles in polyploid tissues. The epithelium of the marine chordate *Oikopleura dioica* is composed of a fixed number of cells grouped in territories according to gene-specific expression and nuclear sizes and shapes. As the animal grows 10-fold during the life cycle, epithelial cells increase in size differentially as a function of their spatial position. We show that this cellular pattern reflected differences in ploidy levels ranging from 34 to 1300 C. The diverse ploidy levels in defined cellular fields resulted both from different timing of entry into endocycles and from cell-specific regulation of endocycle lengths. Throughout the life cycle, differential cell size and ploidy increases were accompanied by field-specific profiles of progressive reductions in G-phase duration. Endocycles were asynchronous among cells of a given epithelial territory, but at the resolution of individual cells, both DNA replication timing and ploidy levels were bilaterally symmetric. The transparent, accessible, oikoplastic epithelium is a model of choice for the study of endoreduplication in the context of pattern formation and growth.

Key Words: **endocycle; urochordate; polyploidisation; Appendicularia; bilateral symmetry.**

INTRODUCTION

Once the body plan has been established, growth of the organism is achieved through the coordinate increase in volume of the different tissues and organs (Conlon and Raff, 1999). In vertebrates, this occurs primarily through spatio-temporal control of cell proliferation. Numerous examples indicate that cell size is constrained by the nucleocytoplasmic ratio (Masui, 1992) and that the final size of an organism, and each of its organs, will be determined by cell numbers. An alternative mechanism, however, is growth through increase in cell size instead of increasing cell number. This strategy seems more widely used in invertebrates, with epidermal growth in *Drosophila* larvae and in rhabditid worms (Edgar and Orr-Weaver, 2001; Flemming *et al.*, 2000) being most extensively studied. In order to respect constraints imposed by the nucleocytoplasmic ratio, an increase in nuclear volume through polyploidisation is probably central to this mechanism. In both nematodes and *Drosophila*, the final ploidy of all cells in the epidermis is globally equivalent, and there appears to be no programmed developmental pattern of cell-specific control of ploidy level (Flemming *et al.*, 2000; Smith and Orr-Weaver, 1991). This overall level of ploidy increase superimposed on the original body plan determines the size of the fly larva and the nematode worm. Control of overall body size via cell growth has thus far not been reported in chordates.

Polyploidisation can result from successive rounds of DNA replication in the absence of karyokinesis or from nuclear fusion in a common cytoplasm. Any cell cycle that bypasses mitosis partially (endomitosis) or completely (endoreduplication) will yield polyploid nuclei. Polyploidisation occurs in most organisms from protists to humans, with considerable diversity in the types of endocycles employed. Polyploidisation is not used extensively in vertebrates, but well-characterised examples of endomitosis include giant murine trophoblasts (MacAuley *et al.*, 1998; Zybina and Zybina, 1996) and human megakaryocytes (Ravid *et al.*, 2002). Polyploidisation among invertebrates is prevalent in secretory tissues and has been best described in *Drosophila*, where a variety of endocyclic mechanisms are used. *Drosophila* polyploid nuclei can be polytene or non-polytene and are found with complete or incomplete DNA

[1] To whom correspondence should be addressed. Fax: +47-55-58-43-05. E-mail: Eric.Thompson@sars.uib.no.

0012-1606/02 $35.00

replication (Dej and Spradling, 1999). Ploidy levels exceeding 24,000 C have been reported in endosperm cells of plants (Traas *et al.*, 1998), but surveys of the literature suggest that it is relatively rare to exceed a few thousand C with values frequently being much lower.

At the molecular level, endoreduplication is poorly understood and how cells attain or exceed ploidies of 1000 C remains essentially uncharacterized. In *Drosophila* (Lilly and Spradling, 1996) and in murine trophoblasts (MacAuley *et al.*, 1998), oscillation of cyclin E activity seems compulsory to reform prereplication complexes and allow firing of replication origins, with gap phases occurring between rounds of replication. Accurate S-phase checkpoint completion of replication is lost in some endocycles, and when DNA content was measured during *Drosophila* and nematode polyploidisation, the first endocyles yielded 4C and 8C, but integral multiples of 2C were subsequently lost (Dej and Spradling, 1999; Flemming *et al.*, 2000), and late firing replication origins were skipped as endoreduplication proceeded. These data suggest that primary control of endocycle progression likely occurs at the onset of S-phase.

In this study using the chordate, Appendicularian, *Oikopleura dioica*, we demonstrate that pattern formation occurs through developmental cell-specific differences in endocycle length. The pelagic, pan-global Appendicularia are the second most abundant component of marine zooplankton after copepods. Appendicularians exploit a wide range of both live and dead organic particles spanning several orders of magnitude in size down to 0.2 μm (Flood and Deibel, 1998). They accomplish this by living inside an elaborate multichambered extracellular house, complete with inlet and food concentrating filters, secreted from the oikoplastic epithelium, a monolayer of transparent cells covering the entire trunk. During the feeding stage of the life cycle of *O. dioica*, houses are constantly discarded and new ones resynthesised every 3–4 h. Oikoplastic cells cease mitotic division prior to metamorphosis and secretion of the first house, and their number is fixed for a given species of *Oikopleura*, being about 2000 for *O. dioica* (Fenaux, 1998; Lohmann, 1899; Spriet, 1997). After metamorphosis, the animal grows about 10-fold in size, and there is a concomitant increase in the size of the oikoplastic cells (Fig. 1). The epithelium consists of multiple cell fields, each with specific size, shape, nuclear morphology, and gene expression pattern related to certain house structures (Spada *et al.*, 2001; Thompson *et al.*, 2001).

Here, we show that development of the epithelium can be divided into three periods. Initially, the epithelium was established through mitotic division of cells during a period in which there was little overall growth of the animal. In a transition phase, prior to metamorphosis, some cells continued to divide mitotically while others entered endocycles as they continued to migrate. At metamorphosis, the number of epithelial cells had become fixed. Further evolution in the patterning and growth of the epithelium occurred entirely through endocycles in which all cells exhibited periods of DNA synthesis (S-phases) separated by gap phases (G-phases) but showed no evidence of partial entry into mitosis (endomitosis). The wide range of field-specific ploidy levels in the epithelium resulted both from asynchronous entry into endocycles and from cell-specific regulation of endocycle length. A contributing factor to formation of the epithelium was a clear bilateral symmetry in both DNA replication timing and ploidy level, suggesting an underlying cell-autonomous clocking mechanism in the patterning and growth of this organ.

MATERIALS AND METHODS

Culture of O. dioica

The source of animals and the culture protocol for *O. dioica* has been previously described (Spada *et al.*, 2001). Briefly, animals were maintained at 15°C in charcoal- and size-filtered (1 μm) seawater in 6-litre beakers with constant slow stirring. Animals were fed twice daily with a mixture of the algal strains *Isochrysis galbana*, *Chaetoceros calcitrans*, and *Rhodomonas* sp. Spawns were set up with 30–40 mature females and 20–30 mature males placed together in 4 litres of seawater. Animals were diluted 1:8 at day 1 and 1:1 at day 2. Subsequently, animals were manually transferred into fresh beakers on a daily basis until maturation and spawning. At 15°C, the average generation time was 160 h (Troedsson *et al.*, 2002); the first mature animals were observed at 5 days and the latest at 7 days. In the case of experiments designed to measure G-phase length, mature animals were added to the spawn over a 10-h period to increase randomisation of developmental stages during subsequent sampling.

For *in vitro* fertilisation, sperm from three to four males was collected in a watch glass and diluted in 50 ml sterile filtered seawater. Aliquots of 2–3 ml of this solution were added to freshly spawned oocytes in sterile filtered seawater in watch glasses. Under these conditions, 50–80% of the eggs divided within 20 min. Tadpoles (premetamorphic) of the desired stage were collected from the watch glasses in which the *in vitro* fertilisations had been carried out. Juveniles (metamorphosis to gamete differentiation) and mature animals (fully developed gonads) were sampled from the running culture.

BrdU Labelling

BrdU (Sigma) was freshly dissolved into filtered seawater and complemented with the required algal cells (BrdU-SW). Final BrdU concentrations used were 50 μM for incubations with tadpoles, and either 100 μM (incubation $>$4 h) or 250 μM (incubation $\leq$ 4h) for later developmental stages. For long-pulse BrdU labelling experiments, 10–20 animals were collected at 24-h intervals and incubated in 1 litre BrdU-SW for 15–20 h. For Gap-phase-length measurement, 40–60 animals were collected at 24-h intervals and incubated in 2 litres BrdU-SW. At defined intervals, samples of 10 animals were fixed and immunostained. Oikoplastic cells of juveniles and adults showed BrdU incorporation after 30 min or 1 h in 250 μM or 100 μM BrdU-SW, respectively. Tadpoles incorporated BrdU after 5–10 min of incubation.

Whole-Mount BrdU Detection

Animals were fixed in 4% paraformaldehyde, 100 mM Mops, 500 mM NaCl, pH 7.5, for 15 min and then washed twice in PBS. All

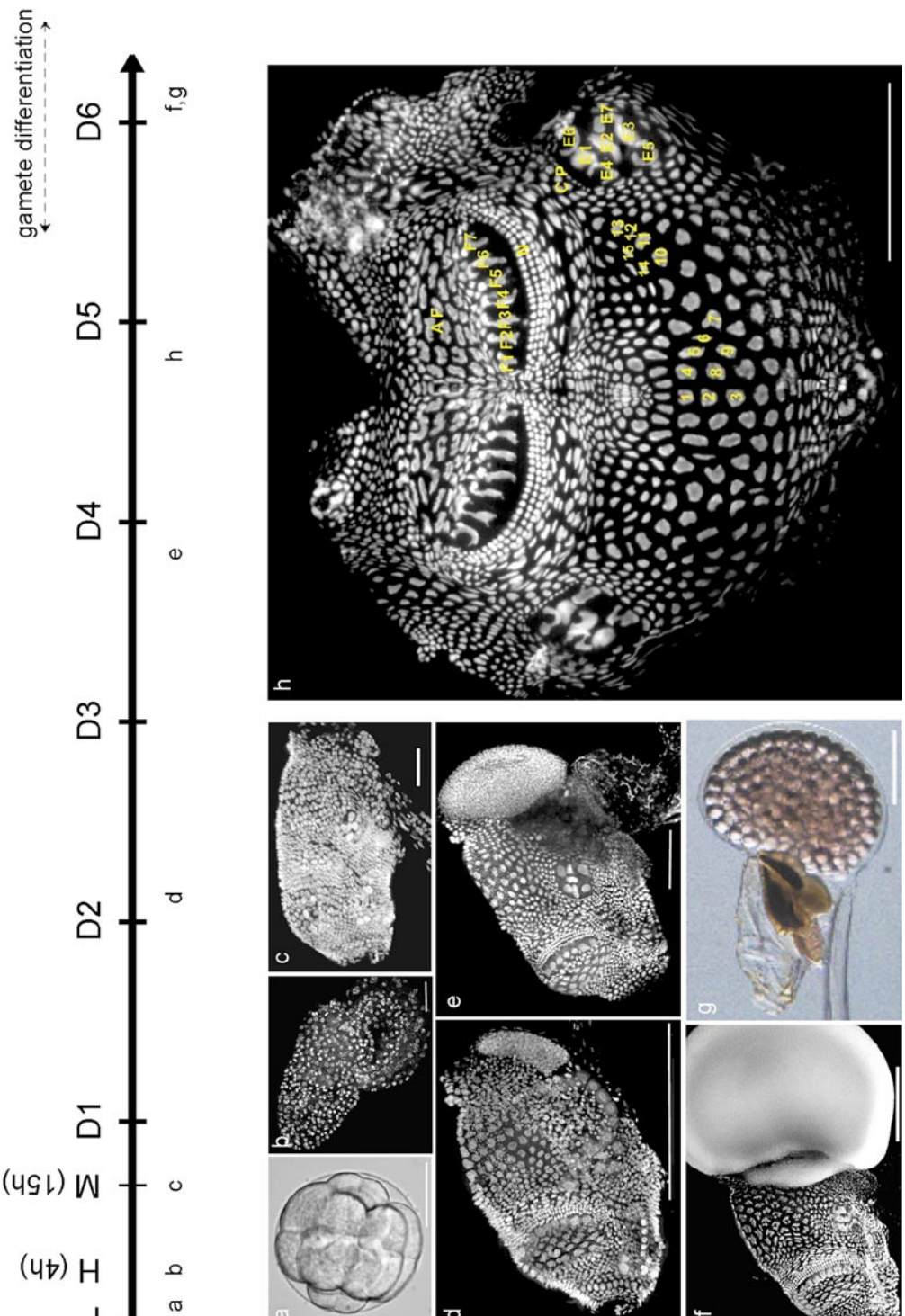

FIG. 1. Oikoplastic epithelium of the urochordate *O. dioica*. Time scale shows chronology of the images below. F, fertilisation; H, hatching at 4 h; M, metamorphosis at 15 h; D1–D6, day 1 to day 6. (a) Fertilised embryos undergo rapid 5- to 10-min division cycles. (b) Tadpoles hatch from the chorion after 4–5 h and show extensive mitotic activity. (c) At 15–16 h, tadpoles undergo metamorphosis, with the tail, retaining the notochord as its axial structure, shifting in position to become orthogonal to the trunk. Cells composing the oikoplastic epithelium are in their final positions and have ceased mitotic division. The animal produces its first house. (d, e) Following metamorphosis, the animal grows about 10-fold and there is a concomitant increase in the size of oikoplastic cells and their nuclei. After 6 days at 15°C, mature males (f) and females (g) spawn and die. The trunk and gonads are transparent throughout the life cycle. (a, g) Phase contrast micrographs. (b–f) Fluorescence micrographs of propidium iodide stained nuclei. (b–g) Anterior to the left, dorsal at the top. (h) Microdissected oikoplastic epithelial spread stained with Hoescht (anterior at top, dorsal–ventral axis is from the midline of bilateral symmetry to the left and right edges of the spread). Different fields of nuclei are recognised by position, shape, and size. These fields have distinct gene expression patterns related to production of diverse house components and have a defined nomenclature (Thompson *et al.*, 2001). Yellow labelling indicates groups of cells central to this study. AF, anterior Fol; F1–F7, 7 giant Fol cells; N, Nasse cells; CP, chain of pearls; E1–E7, 7 giant Eisen cells; 1–15, dorsal cells. Scale bars: 20 μm in (a–c), 100 μm in (d, e), and 250 μm in (f–h).

washing steps were for 5 min at room temperature. With the exception of tadpoles, animals were incubated in 5 μg/ml proteinase K/PBS/0.05% Triton X-100 at room temperature for 3–6 min (depending on animal size). They were then transferred into 4 M HCl for 20 min, washed twice in PBS and then 2 times in 0.5% PBS/0.1% BSA/0.1% Tween 20. They were then blocked in the latter solution for 45 min at room temperature. Immunodetection of BrdU was carried out by using a monoclonal, anti-BrdU-Fluo-antibody (Roche) in the same buffer as the blocking step. Antibody incubation was 30 min at 37°C for tadpoles and 48 h at 4°C for later stages. Animals were then washed once in PBS, placed in PBS/20 μg/ml propidium iodide for 15 min on ice to counterstain nuclei, and washed once more in PBS. Animals were mounted in Vectashield medium (Vector Laboratories) and analysed with a Leica TCS laser scanning confocal microscope equipped with Leica Power-Scan software. Images shown in figures are projections of series of optical sections encompassing the epithelial layer of each animal.

Laser Scanning Cytometry

Preparation of epithelial spreads. Juveniles from day 3 to day 5 and mature animals were collected from the culture over a 6-month period. They were fixed as above, washed twice in PBS/0.1% Tween, and stored on ice prior to microdissection. The oikoplastic epithelium was separated from the rest of the trunk by gently pulling at the tail–trunk junction using tungsten microneedles and then opened ventrally using the same tools. The tail and the gonads were easily separated from the inner organs of the animal. The gut was manually sheared into fragments. Gut fragments and oikoplasts were stored separately in PBS/0.1% Tween on ice. Tissue samples were incubated in PBS/100 μg/ml RNase A (Roche) for 15 min at room temperature, then placed in PBS/propidium iodide (20 μg/ml) for 15 min on ice and finally washed twice in PBS.

Five mature males were forced to spawn, the sperm was collected, and aliquots were checked for motility. Sperm samples were fixed and treated as for microdissected tissues. Zebrafish were sectioned close to the tail fin, and blood was recovered in a drop of PBS/1 mM EDTA. This blood solution was fixed and treated in parallel with the microdissected samples. Single oikoplastic epithelia were carefully spread onto microscope slides in a drop of vectashield and, in the case of spreads from mature animals, prepared zebrafish erythrocytes were added into the same drop. Gut fragments from individual animals were mixed with prepared zebrafish erythrocytes in vectashield and mounted on slides. The same procedure was carried out for sperm samples.

DNA index measurement. Samples were analysed by using a Leica Laser Scanning Cytometer equipped with Win-Cyte 3-3 software (Broegelmann Research Laboratory, University of Bergen, Norway). The instrument offset was set at the same value for all samples. Photomultiplier gain was optimised for each tissue sample, and zebrafish erythrocytes were used to set the DNA index to a value of one. Threshold and background levels were set to define nuclear boundaries, and each nucleus was measured three times on average. Some nuclei of particular fields were unreadable through loss during preparation or because nuclei were juxtaposed and threshold nuclear boundaries could not be set.

RESULTS

DNA Replication throughout the Life Cycle of O. dioica

By the time the tailshift metamorphic event occurs, the definitive number of cells composing the oikoplastic epithelium is fixed (Fig. 1). During the tadpole stage preceding tailshift, cell division occurs throughout most of the epithelium, though some groups of cells, such as the giant Fol and Eisen cells, cease division precociously. From the cleaving embryo up to tailshift, during which the body plan is defined and all organs established, the animal depends on maternal reserves and growth is minimal (Figs. 1a–1c). As the animal grows (Figs. 1c–1h and 2), the nuclear morphology of cells composing different regions of the oikoplastic epithelium becomes increasingly distinctive and size differences between nuclei in different cell subtypes become very apparent. The characteristic sizes and shapes of the nuclei in different cellular fields of the oikoplast develop continuously in a bilaterally symmetric fashion (Figs. 1h and 2). To obtain insight into how this cellular template forms and evolves, DNA replication patterns were examined throughout the life cycle, with particular focus on the groups of cells indicated in Fig. 1h. This was done by using variable BrdU pulses throughout the development of *O. dioica*.

Incubation of animals in long 15- to 18-h pulses of BrdU in seawater revealed DNA replication in all cells of the epithelium from day 1 to day 6 (Fig. 2). At these long incubations, the vast majority of nuclei in the epithelium exhibited complete overlap of BrdU staining and propidium iodide chromatin counterstaining. The change in nuclear size and shape through the life cycle was particularly evident in the giant Fol and Eisen nuclei that increased five- to sixfold in diameter (Figs. 2B and 2C). The time course of BrdU staining showed that this size increase occurred at least in part to accommodate newly synthesized DNA and could not simply be accounted for as a progressive decompaction of chromatin or other rearrangement of nuclear organisation. Thus, all cells of the epithelium underwent replication phases throughout the growth phase without intervening mitoses. To determine when the epithelial cells enter and exit endocycles, animals were exposed to shorter pulses of BrdU (ranging from 20 min to 3 h) during epithelial ontogeny at the tadpole stage, and in animals undergoing gamete differentiation just prior to spawning and death (Fig. 3).

In early tadpoles, 6–7 h postfertilisation, the full complement of epithelial cells was not yet present, but the seven giant Fol and seven giant Eisen cells were identifiable. The migration of these giant cells to their final disposition has been continuously monitored by *in vivo* video microscopy using dilute Hoechst staining of nuclei (Spriet, 1997). At 6–7 h postfertilisation, these cells replicated DNA (Fig. 3I, top row), did not divide any further, and had therefore already entered endocycles. BrdU pulses of 40 min on tadpoles 9 h postfertilisation clearly showed that DNA replication was asynchronous in the epithelium (Fig. 3I, middle row). Furthermore, DNA replication was asynchro-

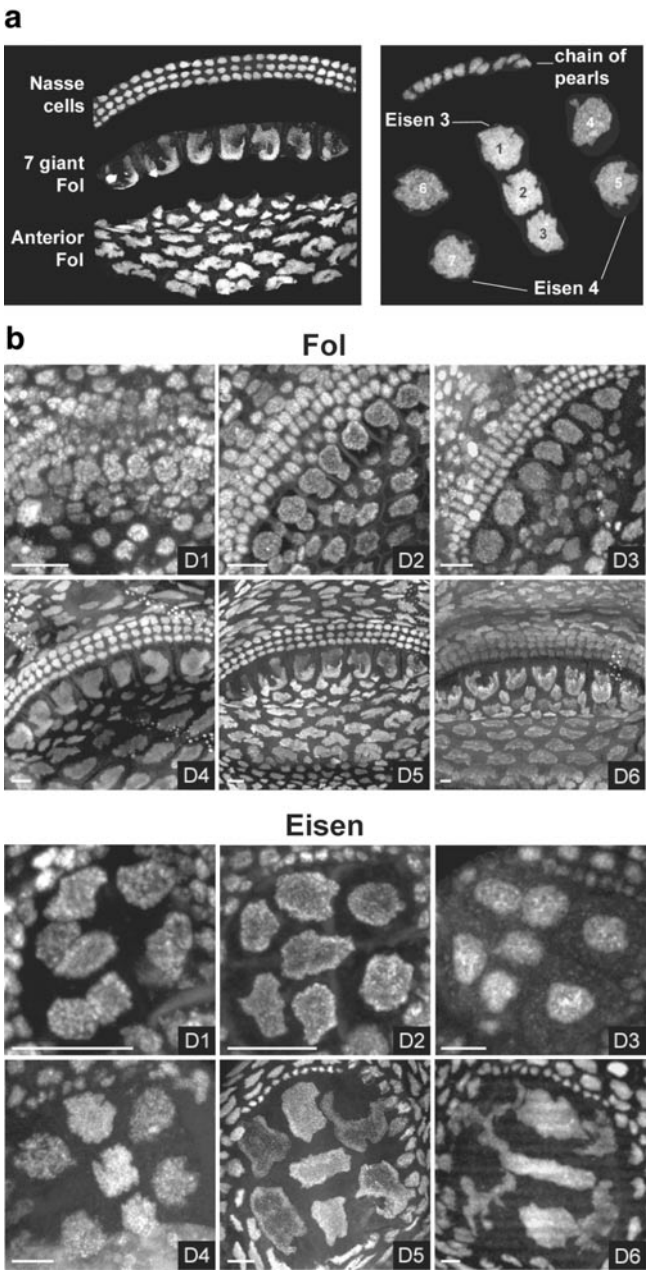

FIG. 2. Oikoplastic cells replicate DNA throughout the growth phase of the life cycle. (A) Expanded images showing propidium iodide-stained nuclei of cells composing the fields of Eisen (right) and Fol (left). The field of Fol is subdivided into the Nasse cells, the seven giant cells, and the anterior cells. The Field of Eisen consists of the chain of pearls and the seven giant cells. Giant Eisen cells are further subdivided into the central Eisen 3 (E1–E3) and the flanking Eisen 4 (E4–E7) based on different chromatin textures and gene expression patterns (Spada *et al.*, 2001). (B) Fluorescence micrographs of day 1–6 animals showing anti-BrdU staining in the fields of Fol and Eisen after exposure of animals to overnight pulses of BrdU. Anti-BrdU staining was entirely coincident with propidium iodide counterstaining with the exception of the nuclei of the chain of pearls that were partially labelled during early stages. Other epithelial fields showed similar results (data not shown). Therefore, DNA replication occurred in all cells of the epithelium throughout the life cycle. The scale bars in all micrographs represent 10 μm, demonstrating the considerable increase in size of individual nuclei from day 1 to day 6. For example, Fol 4 increases in diameter from 5.6 to 28.1 μm from day 1 to day 6, while Eisen 1 increases from 5.2 to 32.3 μm over the same period.

nous within a given field of cells in the epithelium, such as the giant Fol or Eisen cells. Replication patterns remained asynchronous when all epithelial cells were in place after the metamorphic tailshift (Fig. 3I, bottom row).

Near the end of the life cycle, gamete differentiation occurs over a period of 12 h, and the reproductive organ increases rapidly in size to become equivalent to the entire trunk of the animal (Figs. 1f and 1g). Exposure of animals to 3-h BrdU pulses during this period (Fig. 3II), revealed cells in the reproductive organ replicating DNA, but no oikoplastic epithelial cells were observed in S-phase. In fact, the vast majority of cells in all somatic tissues of the animal had ceased DNA replication. The few exceptions consisted of a group of cells located ventrally, just underneath the epithelium, as well as some cells surrounding nervous tissue (co-staining with anti-acetylated tubulin; data not shown) in the anterior ganglion (Fig. 3II, k and l).

Bilateral Symmetry in Temporal Spatial Replication Patterns in the Oikoplastic Epithelium

Throughout growth of the animals, 2- to 4-h-long pulses of BrdU revealed a proportion of nonreplicating cells in each field of the epithelium. At different developmental times, and in different individuals, the positional identity of nonreplicating and replicating cells within a given field changed. Taken together, these results demonstrated the occurrence of gap phases between successive S-phases. In addition to asynchronous endocycles, short-pulse experiments revealed a bilateral symmetry in timing of replication (Fig. 4). This was readily apparent among the right and left groups of giant Fol cells, but was also verified for groups of cells as distant from the central axis as the right and left giant Eisen cells. Bilateral replication symmetry occurred throughout the epithelium, including morphologically more complex regions such as the anterior rosette, and was evident from tailshift through to gamete differentiation.

In addition to the replication patterns, bilateral symmetry was also observed in laser scanning cytometric measurement of the DNA contents of left–right pairs of cells in the oikoplast (Fig. 5A). Each oikoplastic nucleus had a DNA content that was equivalent to its distant bilaterally symmetric partner but could be significantly different from nuclei of its immediate cell neighbours (e.g., dorsal cell 6). Mirror image patterns in DNA content were observed across the entire epithelium from day 3 to maturity (data not shown). The asynchrony of endocycles within a given field of cells was matched by

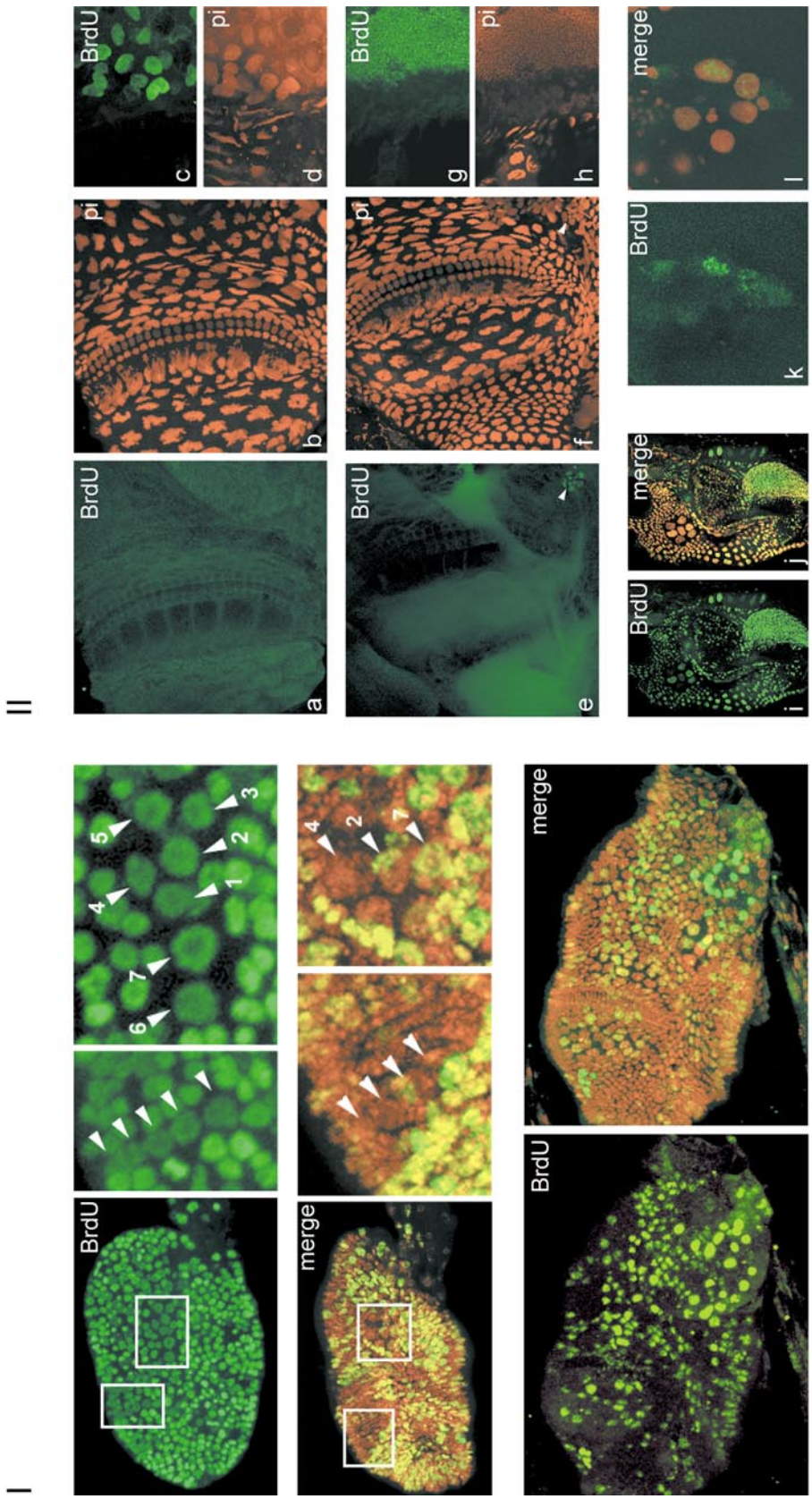

FIG. 3. Endoreduplication begins before tailshift and stops during gamete differentiation. (Panel I, Top row) Anti-BrdU staining of a tadpole 6–7 h postfertilisation following a 20-min BrdU pulse. (Top left) Side view of trunk with inset boxes showing Fol (left) and Eisen (right) regions. (Top middle) Enlargement of Fol region with giant Fol cells indicated by arrowheads. (Top right) Enlargement of Eisen region with numbered arrowheads indicating migrating giant cells not yet positioned in their final 2-3-2 arrangement. All cells of the fully differentiated epithelium are not yet present, but the final complement of giant Fol and giant Eisen cells are present, replicate DNA, and will no longer undergo cell division. (Center row) Anti-BrdU staining superimposed on propidium iodide nuclear counterstaining of a tadpole 9 h postfertilisation following a 40-min BrdU pulse. Left, middle, and right images show the same series of views as the top row. In the Fol and Eisen fields, some giant cells were not replicating (arrowhead 4), whereas others showed partial BrdU staining (arrowheads 2 and 7). (Bottom row) Tail-shifted juvenile showing anti-BrdU staining (1-h pulse) (left) and anti-BrdU staining superimposed on propidium iodide staining (right). All cells comprising the epithelium are now present. Some cells were replicating DNA, while others were not. (Panel II) DNA replication near the end of the life cycle. Animals were incubated 3 h in BrdU during gamete differentiation: (a–d) female; (e–h) male; (i, j) day 3 control animal. (a, c, e, g, i, and k) Anti-BrdU staining in green; (b, d, f, and h) Propidium iodide staining in red; (j, l) Superposed anti-BrdU and propidium iodide staining. In (a) and (e), the photomultiplier gain was increased to the point where faint background staining was visible but no nuclear incorporation of BrdU was detected in the epithelium. In contrast, cells in the gonads of both females (c) and males (g) were clearly stained as were epithelial cells of control day 3 animals (i, j) included in the same experiment. While the vast majority of all cells in the trunk of the animal ceased replication during final maturation, a few small groups of unidentified cells (arrowheads in e, f) as well as cells within the anterior neural ganglion (k, l) continued to replicate DNA.

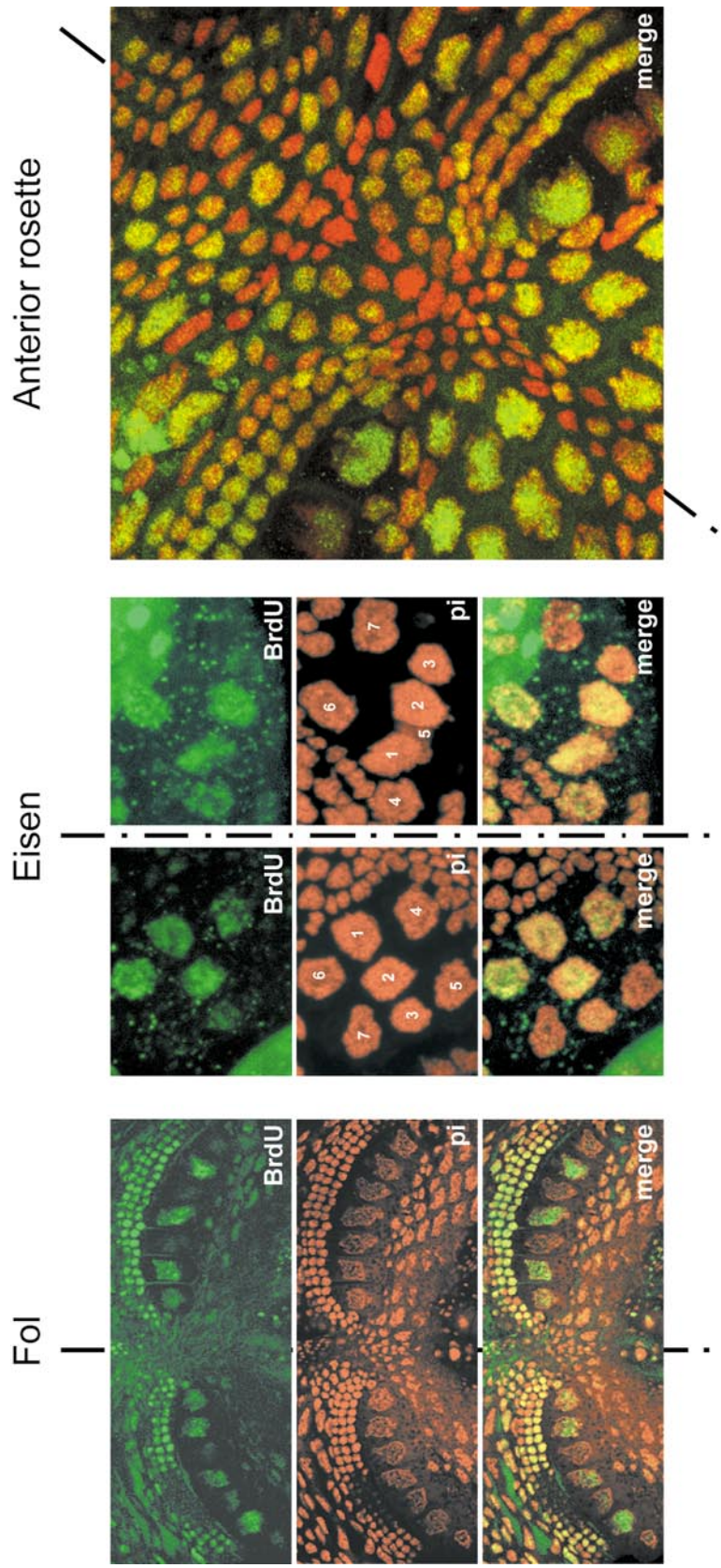

FIG. 4. Endocycles are asynchronous within a given field of oikoplastic cells, but the replication pattern is bilaterally symmetrical. After 2- to 4-h BrdU pulses on day 3–4 animals, anti-BrdU staining (BrdU, green), propidium iodide nuclear counterstaining (pi, red), and superposed images (merge) were obtained. (Left panel) Dorsal view with the left and right fields of Fol shown. On each side, the giant cells F1, F2, F4, and F6 are BrdU-positive at similar levels, whereas F3, F5, and F7 are only faintly stained. (Middle panel) Left and right fields of Eisen. Giant cells E5 and E7 were not replicating on either side contrary to E1, E2, E4, and E5, which showed strong BrdU incorporation on both sides (numbering of giant Eisen cells is indicated on the propidium iodide images). The E3 giant cell showed intermediate staining on both sides. (Right panel) View of the anterior rosette showing that bilateral symmetry in oikoplastic epithelial replication patterns was not restricted to giant Fol and Eisen cells.

a

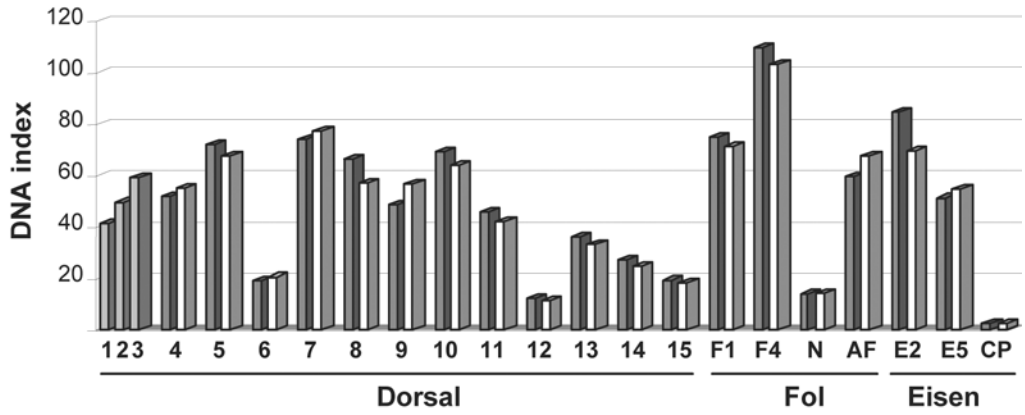

b

Stage	Giant Fol Cells							
	F1	F2	F3	F4	F5	F6	F7	Max
M	**1.00**	**1.19**	**1.44**	**1.53**	**1.47**	**1.48**	**1.12**	2.00
(7)	0.00	0.09	0.08	0.09	0.08	0.10	0.12	F6
D5	**1.00**	**1.48**	**1.62**	**1.83**	**1.88**	**1.77**	**0.98**	2.32
(4)	0.00	0.08	0.19	0.13	0.19	0.13	0.09	F4
D4	**1.00**	**1.64**	**2.06**	**2.25**	**1.64**	**2.00**	**1.44**	3.39
(6)	0.00	0.13	0.16	0.57	0.15	0.32	0.24	F4
D3	**1.00**	**1.23**	**1.12**	**1.37**	**1.12**	**1.62**	**1.12**	1.63
(3)	0.00	0.08	0.06	0.15	0.09	0.12	0.12	F6

Stage	Giant Eisen Cells			
	E1	E2	E3	Max
M	**1.22**	**1.30**	**1.00**	1.53
(6)	0.06	0.03	0.00	E1
D5	**1.45**	**1.50**	**1.00**	1.92
(2)	0.04	0.05	0.00	E1
D4	**1.28**	**1.42**	**1.00**	1.63
(6)	0.12	0.07	0.00	E2
D3	**1.20**	**1.41**	**1.00**	1.89
(4)	0.10	0.16	0.00	E2

Stage	Cell Type			
	CP	Nasse	AF	Gut
M	**2.05**	**1.96**	**1.86**	**2.09**
	8	14	17	28
D5	**nd**	**1.82**	**2.06**	**2.11**
		25	29	16
D4	**nd**	**1.77**	**2.25**	**2.53**
		22	8	39
D3	**1.73**	**1.60**	**1.47**	**2.33**
	8	6	7	29

FIG. 5. Epithelial ploidy levels are bilaterally symmetrical but not homogenous within a given field of functionally related cells. (A) Relative DNA content of cells in various fields of the oikoplastic epithelium (see nomenclature Fig. 1B) measured from a mature female. At this developmental stage, DNA replication no longer occurs in the epithelium. Bars in dark gray and white correspond to cells from the left and right sides of the animal, respectively. Dorsal cells 1–3 (lighter gray bars) are on the axis of symmetry and do not occur as right–left pairs. The DNA index values are given relative to zebrafish erythrocytes spread on the same slide. N, Nasse cells; AF, anterior Fol cells; CP, chain of pearl cells. (B) Evolution of relative DNA contents from day 3 to maturity. Prior to day 3, it was not technically feasible to make epithelial spreads for laser scanning cytometry because of the small size of the animals. Stages: M, mature; D3–D5, day 3–5. Numbers in parentheses indicate the number of epithelial fields quantified. For the giant Fol and Eisen cells, DNA contents were normalised to the right F1 giant cell of Fol and the left E3 giant cell of Eisen, respectively. Standard errors are in smaller type below the values. At each stage, the maximum amplitude in relative DNA content within a field is indicated in the "Max" column with the cell attaining this level indicated directly below the amplitude value. In the lower right table, the maximum relative difference in DNA content at each stage, within a specified cell type, is given for the chain of pearl cells (CP), the Nasse cells and the anterior Fol cells (AF), as well as for cells lining the gut. These latter cells lining the digestive tract are diploid (Fig. 6). The number of cells examined at each stage, for each field, is given in smaller type below the maximum amplitude value. These values show that, with few exceptions, the cells of a specific field were consistently within one cell cycle of each other.

a Sperm (haploid)

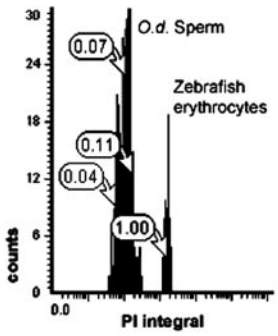

b Gut cells (diploid)

Stage	Ploidy distribution (%)				
	1C	2C	3C	4C	5C
M	0	30	60	10	0
D5	0	0	73	20	7
D4	0	13	49	37	1
D3	0	7	71	22	0

c Oikoplastic epithelium (polyploid)

Cell Type		Ploidy (C)	SE
Giant Fol:	Mean	1088	92
	F1	831	68
Giant Eisen:	Mean	1308	551
	E3	1076	183
Chain of Pearls		34	1
Nasse		180	3
Anterior Fol		782	25
Dorsal:	1	686	47
	2	933	111
	3	1015	86
	4	1079	208
	5	1139	73
	6	289	52
	7	1165	41
	8	1016	80
	9	932	92

FIG. 6. DNA content of diverse cells in mature animals. (A) Determination of haploid DNA index value for *O. dioica* sperm using zebrafish erythrocytes for calibration. Setting zebrafish erythrocyte nuclei to a DNA index (DI) of 1.0 yielded a peak value of 0.07 of *O. dioica* sperm in a flow cytometric analysis. In a second approach, manual counting of individual sperm was done by laser scanning cytometry, again with zebrafish erythrocyte nuclei set to a DI of 1.0. The mean value obtained for *O. dioica* sperm after 5 independent experiments with a total sample count of 146 individual sperm was 0.074 ± 0.018. In all subsequent measurements of ploidy of nuclei of different cell types in *O. dioica*, the zebrafish erythrocyte nucleus standard was set to a DI of 1.0, and ploidy (C = haploid equivalents) was calculated as C = (DI of measured cell nucleus)/0.07. (B) Ploidy distribution of proliferating cells lining the digestive tract. The distribution of ploidy values was consistently between 2C (G1) and 4C (G2), in agreement with these cells being diploid. M, mature; D3–D5, day 3–5. (C) Cells of the oikoplastic epithelium are polyploid. Ploidy values were determined for diverse groups of cells in the oikoplastic epithelium (see nomenclature Fig. 1h) in mature animals. Standard errors are given in the column "SE.". For giant Fol and Eisen cells, ploidy is given for reference nuclei F1 and E3 (Figs. 1h and 5B) as well as a mean value for all cells in the giant Fol and Eisen fields.

heterogeneity in DNA contents (Fig. 5B). For example, among giant Fol cells, F1 and F7 had lower DNA content than F4–F6. This was true both of mature animals when DNA replication had ceased in the epithelium and in day 3–5 animals undergoing endoreplication. In general, however, at a given point in time, the relative DNA contents within a specific epithelial cell type did not vary by more than a factor of two. This suggests that all cells of a given field were within one endocycle of each other. A parsimonious explanation for the observed heterogeneity would then be that, for example, giant Fol F4–F6 cells were always advanced in the endocycle relative to F1 and F7. An alternative, more complex explanation would be that the genome was differentially amplified, even among cells of the same field.

Ploidy Level and G-Phase Length Are Negatively Correlated

To determine the final ploidy levels attained in *O. dioica*, we measured the DNA index of diverse types of cells in mature animals against zebrafish erythrocytes as a calibration standard (Fig. 6). Cells lining the digestive tract divided continuously and had C values two to four times that of sperm cells (Fig. 6B) as expected for diploid cells traversing G_1, S-, and G_2 phases. On the other hand, all oikoplastic epithelial cells were polyploid (Fig. 6C). In mature animals, final ploidy levels ranged from a low of 34 C in chain of pearl nuclei to 1300 C in giant Eisen nuclei. These variations may reflect cell lineage differences in the number of endocycles and/or variable extents of genome replication.

To evaluate these possibilities, BrdU labelling experiments were conducted to characterise endocycle lengths throughout the life cycle (Fig. 7). In an asynchronous population of cells, G-phase duration is defined as the longest BrdU pulse length at which some cells still do not show incorporation. In all cell fields examined, G-phase length shortened progressively throughout the life cycle. We also observed that G-phase was always significantly shorter in cells attaining high ploidy levels such as giant Fol and Eisen cells than it was in those with more modest ploidy levels such as the chain of pearl and Nasse cells (Table 1).

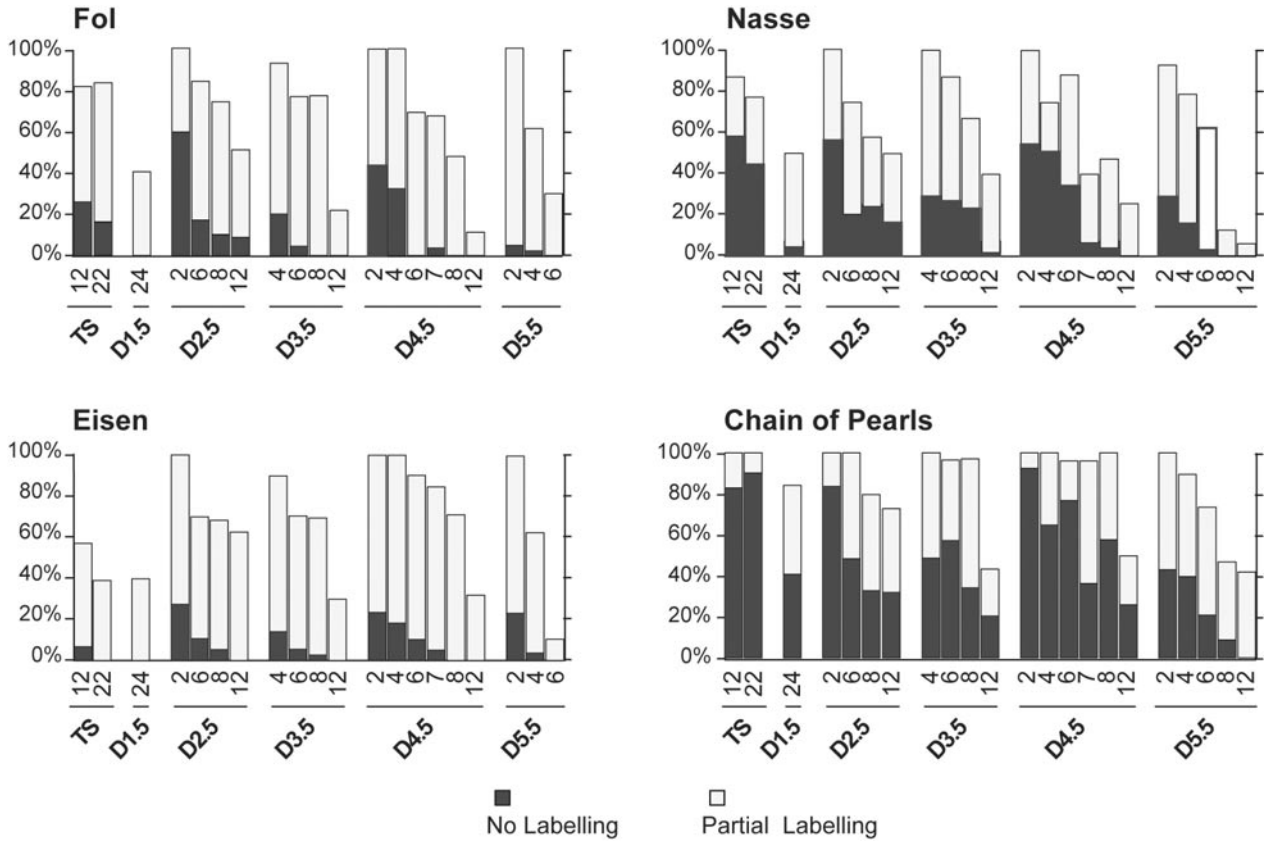

FIG. 7. Epithelial growth is accompanied by cell type-specific reduction in Gap-phase length. Animals from the same generation were subjected to varying BrdU pulse lengths (hours on the abscissa) from metamorphic tailshift (TS) through to day 5.5 (D5.5). For each pulse length, 10 animals were examined for BrdU incorporation. Confocal analysis was performed for the 7 giant Fol cells, the 3 central giant Eisen cells, the Nasse cells, and the chain of pearls. Labelling was classified as absent (dark bars, G-phase) or partial (light bars, S-phase). The remaining unclassified nuclei showed almost complete overlap of anti-BrdU labelling and propidium iodide counterstaining and were therefore either nearing completion of S phase or had completed S phase. For most pulse lengths, more than 100 giant Fol, giant Eisen, and chain of pearl nuclei, and more than 800 Nasse nuclei were analysed. All cell types examined showed a decrease in G-phase length through development. G-phase was consistently shorter in giant Fol and Eisen cells than in Nasse and chain of pearl cells.

If G-phase length shortens, then the duration of the endocycles would also shorten unless there was a compensatory lengthening of S-phase. In the cell fields examined, inspection of Table 1 reveals that this would require an extension of the S-phase by more than 20 h between days 2 and 6. This was not the case. The shortest BrdU pulse lengths required to observe the first cells with completely coincident anti-BrdU staining and propidium iodide counterstaining among giant Fol or Eisen cells never exceeded 6–8 h. Furthermore, the downward slopes in the proportions of partially labelled nuclei with increasing pulse length on different days (Fig. 7) paralleled the downward slopes in the proportions of G-phase cells and did not show any compensatory opposite upward trend. Finally, extension of S-phase from 6 to 8 h to greater than 1 day would mean that it would make the detection of cells in G-phase very unlikely, even at short BrdU pulse lengths, and this was not observed. Therefore, since shorter G-phases were not compensated by corresponding increases in S-phase duration, the overall length of each endocycle progressively shortened. Although we cannot exclude that differential amplification of the genome might occur in different fields of cells, the different endocycle lengths resulting from

TABLE 1

Decreases in Gap-phase Duration fo Epithelial Cells throughout the Life Cycle

	Gap-phase duration (h)					
Cell type	D1	D2	D3	D4	D5	D6
Giant Fol	>22	<24	12	8	6–7	4
Giant Eisen	12–22	<24	8	8	7	4
Nasse	⩾22	24	>12	8–12	8	6
Chain of Pearls	⩾22	>24	⩾12	>12	>12	8

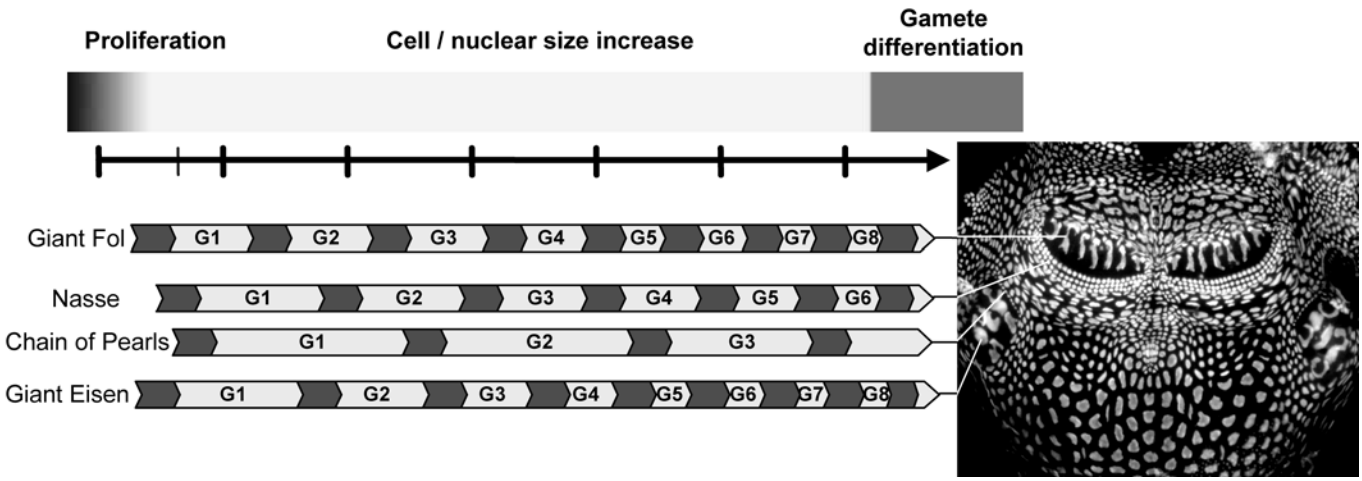

FIG. 8. Proposed model for growth of the oikoplastic epithelium of *O. dioica* by differential polyploidisation of the component cellular fields. Along the time scale arrow, thick bars represent daily intervals and the thin bar indicates the tail shift metamorphic event. During early cleavage and posthatching tadpole stages, the animal develops principally through cellular division. Prior to metamorphosis, some cells, such as the giant Fol and Eisen, are already present in their final number. At this stage, the final fixed number of cells composing the oikoplastic epithelium has not yet been attained. As the giant cells are already replicating DNA during this period, they at least have entered into endocycles prior to metamorphosis. Following tailshift, the oikoplast grows strictly through increases in cell size. Distinct cellular fields grow through a cell type-specific number of endocycles, each characterised by progressive shortening of Gap phases (white arrows) separating successive S-phases (dark arrows). Apart from the row of cells along the axis of bilateral symmetry, each cell on one side of the animal has a counterpart on the other side that follows a mirror image endoreduplication pattern both with respect to timing of DNA replication and ploidy level. Final epithelial ploidy levels range from 34 C for the chain of pearls to over 1000 C for the giant cells of Fol and Eisen.

differential G-phase duration is sufficient to account for the diverse final epithelial ploidy levels (Fig. 8).

DISCUSSION

The tendency to focus research on polyploidisation to a few standard model organisms has led to a fragmentary view of the role that endoreplication plays in pattern formation and growth during development. Among plants, polyploidy appears prevalent in species with small genomes, suggesting a requirement for some aspects of plant growth or function (De Rocher *et al.*, 1990). In *Arabidopsis*, the extent of endoreplication in some cell types may be developmentally programmed, but increased DNA content is also affected by environmental factors such as light (Traas *et al.*, 1998). *Drosophila* embryonic endocycles occur in patterned, tissue-specific domains at defined developmental times (Smith and Orr-Weaver, 1991), but in larvae, where endocycles are extensively employed to assure rapid growth, patterned endoreplication has not been reported and endocycles are asynchronous within tissues (Lilly and Spradling, 1996; Smith and Orr-Weaver, 1991). The adult moth, *Ephestia*, does show patterning over a limited ploidy range (8–32C) in producing different scale sizes on the wing surface (Edgar and Orr-Weaver, 2001). Here, we show that extensive use of polyploidisation can be extended to the chordate phylum. The complex pattern of cellular fields in the oikoplastic epithelium reflected a spatial diversity of final ploidy levels over a 38-fold range. This pattern was achieved by differences in both timing of entry into endoreplication and in the length of ensuing endocycles in different cellular fields.

Polyploidisation was not restricted to the oikoplastic epithelium and occurred in most tissues of *O. dioica* (unpublished data). In the epithelium, long BrdU pulses resulted in complete overlap of anti-BrdU staining and propidium iodide counterstaining of chromatin throughout the life cycle. This suggests that DNA replication was complete during each endocycle, but the resolution of the technique is insufficient to be definitive. The number of endocycles completed in each cellular field (Fig. 8) was consistent with final respective ploidy levels, but the possibility that differential amplification of the genome in the different fields may contribute to the differential ploidy levels cannot be excluded.

Asynchrony of entry into endocycles was integral to the patterning of the oikoplastic epithelium. Giant Fol and Eisen cells attaining the highest final ploidies were also among the earliest cells to enter endocycles. Without exception, there was also asynchrony in the timing of DNA replication within a given field of cells. These asynchronous aspects of epithelial endocycles were in contrast to the abrupt shut down of epithelial DNA replication during the latter phases of gamete differentiation and to bilateral symmetry in replication patterns at the level of left–right pairs of individual cells.

It is of interest to compare developmental patterns of

endocycles in the oikoplastic epithelium of *Oikopleura* to those of both mitotic and endocycles in *Drosophila* and *Caenorhabditis elegans*. Timing of cell proliferation and growth is often critical in determining cell fates, and this has been extensively demonstrated in the heterochronic mutants of *C. elegans* (Ambros, 2000). One key question is to what extent control of timing is cell- or lineage-autonomous vs to what degree it is influenced by cell–cell interactions or responses to gradients or environmental factors. In *Drosophila* imaginal discs, DNA replication occurs in small nonclonal clusters of cells, suggesting that local intercellular communication may have a role in cycle regulation (Bryant, 1996; Milan *et al.*, 1996). On the other hand, during differentiation of the vulva in *C. elegans*, vulval cell divisions were unaffected by ablation of surrounding cells (Kimble, 1981), supporting a cell intrinsic mechanism of cycle timing. With respect to endocycles, the spatial–temporal patterning of endocycles in *Drosophila* embryos followed by the loss of such patterning in larvae led to consideration of the fly embryo as a special case of synchronous endocycle control (Edgar and Orr-Weaver, 2001). The present study demonstrates that synchronous control of endocycles is not restricted to *Drosophila* or to embryonic stages of development. The bilateral replication symmetry in *Oikopleura* is more easily explained through cell lineage-autonomous clocking of cycles than local cell–cell interactions. In this regard, the related urochordate ascidians have been considered a classic example of mosaic cell-autonomous development, though more recently, cell interactions have also been shown to play a significant role (Wolpert, 1998). Thus, cell-autonomous clocking of cell cycles in pattern formation and growth of the oikopleurid epithelium is perhaps not surprising.

In analysing pattern formation, there is also the relationship of cell division to both cell and organismal growth to consider. Despite several possible mechanisms through which cell division could promote cellular growth (Neufeld *et al.*, 1998), little evidence supports such a model. Instead, the prevailing view is that cell growth drives cell cycle progression, though apparent exceptions do exist (Conlon *et al.*, 2001). Mitotic and endoreplicating *Drosophila* larval cells respond differently to nutritional levels and ectopic expression of cell cycle regulators (Britton and Edgar, 1998). When nutrition is withdrawn, mitotic cells continue to proliferate, whereas endocycling cells become quiescent. Conversely, when cyclin E or E2F transcription factors are ectopically expressed in nutritionally deprived larvae, quiescent endoreplicating cells are driven into S-phase, while quiescent mitotic cells are not. The potential relationship between nutrition and control of endocycle progression is particularly intriguing in the oikoplastic epithelium of *Oikopleura*, because it is the epithelium itself that produces the extracellular structure allowing the animal to feed. As the epithelium and the animal grow, the size of the filter-feeding houses increases in parallel, as does the capacity for increased nutrient ingestion. Coincidentally, during this period of growth, in all cellular fields of the epithelium examined, G-phase length decreased concomitantly. Thus, as the capacity for nutritive input increased in concert with the growth of the animal, the frequency of endocycles increased and nuclear ploidy levels rose. The patchwork of polymorphic polyploidisation in the diverse oikoplastic fields adds a further level of complexity in regulating the interaction between cell growth and endocycle progression.

At a larger scale, it has generally been conceded that variation in metazoan body size can essentially be explained by differences in cell number (Wilson, 1925). However, it cannot be excluded that cell size also influences body size in taxa such as nematodes and insects where organisms are often quite small. The relative importance of cell proliferation, endoreduplication, and haploid genome size has been explored in the evolution of nematode body size among species varying between 0.5 and 3.0 mm in length (Flemming *et al.*, 2000). The conclusion was that the final ploidy of hypodermal nuclei, combined with their number, accounted for most of the variation in mature body size. Increased cell size/nuclear ploidy may also contribute to body size regulation in the chordate oikopleurids. Oikopleurid species ranging from 1.3 to 6.5 mm in adult trunk size (Flood and Deibel, 1998) vary between 1600 and 2600 oikoplastic cells arranged in patterns of juxtaposed territories similar to that of *O. dioica* (Spriet, 1997). There is no correlation between cell number and final body size; the species with 1600 cells in the epithelium has an intermediate size of 3.0 mm, whereas the largest species has an intermediate cell number of 1900.

In *C. elegans*, the bone morphogen protein (BMP) family has been implicated in the control of body length. Disruption of the BMP-like pathway did not change the number of nuclei in the nematode hypodermis but did affect the overall level of polyploidisation (Flemming *et al.*, 2000; Morita *et al.*, 2002; Suzuki *et al.*, 1999). In *Drosophila*, the BMP-2/4 homologue, decapentaplegic pathway also influences wing imaginal disk size partially through cell size regulation (Edgar and Lehner, 1996). During our experiments, three natural variants of the giant Fol field were observed, in which each animal had one normal field of seven cells, whereas the opposite field exhibited additional or reduced cell numbers. The variant fields occupied the same physical area as their counterpart normal fields, indicating that the giant Fol territory was defined in space, regardless of the number of constituent cells. The accessibility of the epithelium, the number of juxtaposed territories, and the cellular resolution at which they are defined provide interesting avenues for exploration of mechanisms defining territorial boundaries.

Regulation of organ and body size, and the contributions that control of cell proliferation and cell growth make to this process, are poorly explored areas of developmental biology that have begun to be the subject of more in depth research. The extreme diversity of body sizes and shapes found in nature, even among closely related species, argue against a profound understanding based on a few selected standard model organisms. The estimated genome size of

O. dioica (70 Mb; Seo *et al.*, 2001) is smaller than that of the nematode *C. elegans*, and genome sequencing is currently underway. The very short generation time (5–6 days at 15°C, 1–2 days at 29°C) and high fecundity (>300 oocytes per female) offer favourable perspectives for genetic approaches. Thus, pattern formation in the transparent oikoplastic epithelium of the chordate *Oikopleura* provides an attractive complement, and phylogenetic extension, to studies of these mechanisms in *Drosophila* and *C. elegans*.

ACKNOWLEDGMENTS

We thank Jean-Marie Bouquet for help with culturing animals, Endy Spriet for technical advice on preparing epithelial spreads and for photographs (Figs. 1g and 1h), Roland Jonsson and Maria Ohlsson for assistance with the laser scanning cytometer, and Daniel Chourrout for critical reading of the manuscript. This work was supported by grants from the Norwegian Research Council and Ministry of Education.

REFERENCES

Ambros, V. (2000). Control of developmental timing in *Caenorhabditis elegans*. *Curr. Opin. Genet. Dev.* **10,** 428–433.

Britton, J. S., and Edgar, B. A. (1998). Environmental control of the cell cycle in *Drosophila*: Nutrition activates mitotic and endoreplicative cells by distinct mechanisms. *Development* **125,** 2149–2158.

Bryant, P. J. (1996). Cell proliferation control in *Drosophila*: Flies are not worms. *Bioessays* **18,** 781–784.

Conlon, I., and Raff, M. (1999). Size control in animal development. *Cell* **96,** 235–244.

Conlon, I. J., Dunn, G. A., Mudge, A. W., and Raff, M. C. (2001). Extracellular control of cell size. *Nat. Cell Biol.* **3,** 918–921.

De Rocher, E. J., Harkins, K. R., Galbraith, D. W., and Bohnert, H. J. (1990). Developmentally regulated systemic endopolyploidy in succulents with small genomes. *Science* **250,** 99–111.

Dej, K. J., and Spradling, A. C. (1999). The endocycle controls nurse cell polytene chromosome structure during *Drosophila* oogenesis. *Development* **126,** 293–303.

Edgar, B. A., and Lehner, C. F. (1996). Developmental control of cell cycle regulators: A fly's perspective. *Science* **274,** 1646–1652.

Edgar, B. A., and Orr-Weaver, T. L. (2001). Endoreplication cell cycles: More for less. *Cell* **105,** 297–306.

Fenaux, R. (1998). Life history of the appendicularia. In "The Biology of Pelagic Tunicates" (Q. Bone, Ed.), pp. 151–159. Oxford Univ. Press, New York.

Flemming, A. J., Shen, Z. Z., Cunha, A., Emmons, S. W., and Leroi, A. M. (2000). Somatic polyploidization and cellular proliferation drive body size evolution in nematodes. *Proc. Natl. Acad. Sci. USA* **97,** 5285–5290.

Flood, P., and Deibel, D. (1998). The appendicularian house. In "The Biology of Pelagic Tunicates" (Q. Bone, Ed.), pp. 105–124. Oxford Univ. Press, New York.

Kimble, J. (1981). Alterations in cell lineage following laser ablation of cells in the somatic gonad of *Caenorhabditis elegans*. *Dev. Biol.* **87,** 286–300.

Lilly, M. A., and Spradling, A. C. (1996). The *Drosophila* endocycle is controlled by Cyclin E and lacks a checkpoint ensuring S-phase completion. *Genes Dev.* **10,** 2514–2526.

Lohmann, H. (1899). Das gehäuse der Appendicularien, sein bau, sein funktion und sein entstehung. *Schriften des naturwissenschaftlichen vereins für schleswig-holstein* **11,** 347–407.

MacAuley, A., Cross, J. C., and Werb, Z. (1998). Reprogramming the cell cycle for endoreduplication in rodent trophoblast cells. *Mol. Biol. Cell* **9,** 795–807.

Masui, Y. (1992). Towards understanding the control of the division cycle in animal cells. *Biochem. Cell Biol.* **70,** 920–945.

Milan, M., Campuzano, S., and Garcia-Bellido, A. (1996). Cell cycling and patterned cell proliferation in the *Drosophila* wing during metamorphosis. *Proc. Natl. Acad. Sci. USA* **93,** 11687–11692.

Morita, K., Flemming, A. J., Sugihara, Y., Mochii, M., Suzuki, Y., Yoshida, S., Wood, W. B., Kohara, Y., Leroi, A. M., and Ueno, N. (2002). A *Caenorhabditis elegans* TGF-beta, DBL-1, controls the expression of LON-1, a PR-related protein, that regulates polyploidization and body length. *EMBO J.* **21,** 1063–1073.

Neufeld, T. P., de la Cruz, A. F., Johnston, L. A., and Edgar, B. A. (1998). Coordination of growth and cell division in the *Drosophila* wing. *Cell* **93,** 1183–1193.

Ravid, K., Lu, J., Zimmet, J. M., and Jones, M. R. (2002). Roads to polyploidy: The megakaryocyte example. *J. Cell Physiol.* **190,** 7–20.

Seo, H. C., Kube, M., Edvardsen, R. B., Jensen, M. F., Beck, A., Spriet, E., Gorsky, G., Thompson, E. M., Lehrach, H., Reinhardt, R., and Chourrout, D. (2001). Miniature genome in the marine chordate *Oikopleura dioica*. *Science* **294,** 2506.

Smith, A. V., and Orr-Weaver, T. L. (1991). The regulation of the cell cycle during *Drosophila* embryogenesis: The transition to polyteny. *Development* **112,** 997–1008.

Spada, F., Steen, H., Troedsson, C., Kallesøe, T., Spriet, E., Mann, M., and Thompson, E. (2001). Molecular patterning of the oikoplastic epithelim of the larvacean tunicate *Oikopleura dioica*. *J. Biol. Chem.* **271,** 20624–20632.

Spriet, E. (1997). Studies on the house building epithelium of oikopleurid appendicularia (Tunicata): Early differentiation and description of the adult pattern of oikoplastic cells. Cand. Sci. Thesis, University of Bergen, 57 pp.

Suzuki, Y., Yandell, M. D., Roy, P. J., Krishna, S., Savage-Dunn, C., Ross, R. M., Padgett, R. W., and Wood, W. B. (1999). A BMP homolog acts as a dose-dependent regulator of body size and male tail patterning in *Caenorhabditis elegans*. *Development* **126,** 241–250.

Thompson, E. M., Kallesøe, T., and Spada, F. (2001). Diverse genes expressed in distinct regions of the trunk epithelium define a monolayer cellular template for construction of the oikopleurid house. *Dev. Biol.* **238,** 260–273.

Traas, J., Hulskamp, M., Gendreau, E., and Hofte, H. (1998). Endoreduplication and development: Rule without dividing? *Curr. Opin. Plant Biol.* **1,** 498–503.

Troedsson, C., Bouquet, J.-M., Aksnes, D. L., and Thompson, E. M. (2002). Resource allocation between somatic growth and reproductive output in the pelagic chordate, *Oikopleura dioica*, allows opportunistic response to nutritional variation. *Mar. Ecol. Prog. Ser.*, in press.

Wilson, E. B. (1925). "The Cell in Development and Heredity," pp. 97–99. Macmillan, New York.

Wolpert, L. (1998). "Principles of Development." Oxford Univ. Press, New York.

Zybina, E. V., and Zybina, T. G. (1996). Polytene chromosomes in mammalian cells. *Int. Rev. Cytol.* **165**, 53–119**.**

Received for publication May 28, 2002
Revised August 30, 2002
Accepted August 30, 2002
Published online October 24, 2002